Journal of Geophysical Research-Oceans

Supporting Information for

Enriched Regions of ^{228}Ra along the U.S. GEOTRACES Pacific Meridional Transect (GP15)

Willard S. Moore[1], Matthew A. Charette[2], Paul B. Henderson[2], Douglas E. Hammond[3], Nathaniel Kemnitz[3], Emilie LeRoy[4], Eun Young Kwon[5], Mikael Hult[6]

[1]School of Earth, Ocean & Environment, University of South Carolina, Columbia, SC, USA

[2]Woods Hole Oceanographic Institution, Woods Hole, MA, USA

[3]Department of Earth Sciences, University of Southern California, Los Angeles, CA. USA

[4]UMR 6539 LEMAR, CNRS, IRD, Ifremer, University of Brest, 29280 Plouzane, France

[5]Center for Climate Physics, Institute for Basic Science, Busan, South Korea

[6]European Commission, Joint Research Centre (JRC), Geel, Belgium

Corresponding author: Willard Moore (moore@geol.sc.edu)

Contents of this file

Figures

Introduction:

Here we

1. Provide the analytical procedure for ^{226}Ra measurements.
2. Describe data analysis programs used to develop the data set and estimate uncertainties.
3. Methods used for reporting ^{228}Ra data
4. Matlab code for processing RaDeCC data
5. Measurement of ^{228}Ra on B cartridges
6. Use published data to published data to illustrate how we use ^{228}Ra to estimate the speed of the North Pacific Current.
7. Use the distribution of ^{223}Ra at Puna Ridge to estimate vertical mixing rates.
8. Show depth profiles for each station.
9. References

1. Analysis of ^{226}Ra in 15-25 liter samples to determine ^{228}Ra recovery efficiency

The 15 g Mn-fiber samples from the Niskin were partially dried, placed into a glass equilibrator and flushed with He. After the ^{226}Ra on the Mn-fiber had partially equilibrated with ^{222}Rn (1-4 weeks), the ^{222}Rn was extracted in a vacuum line, transferred to a scintillation cell and the cell was measured by a PMT (Key et al., 1979; Charette et al., 2015). Measurements were typically repeated two times or until the results agreed to within 10%. The Mn-cartridge scavenging efficiency was determined by multiplying the activity ratio of [^{226}Ra on cartridge/^{226}Ra on small volume fiber] by [water volume used for fiber/water volume pumped through cartridge].

2. Least squares fit to the data in Microsoft Excel using the Bateman equation.

Objective: Least squares fit to Bateman Equ. for decays of ^{228}Ra and daughters to the ^{220}Rn isotope that is measured.

Equation Form
Y = a1*x1 + a2*x2 + a3*x3
Where a1 = (^{228}Ra)$_0$, a2 = (^{228}Th)$_0$, a3 = (^{224}Ra)$_0$ and Y = ^{220}Rn activity measured and x1, x2, x3 are functions of time elapsed since sample collection

Samples are run at various times, and the terms for xi are computed from the Bateman eq.
x1 = (1.50079*exp(-3.3e-4*t)-1.50607*exp(-9.925e-4*t)+5.2777e-3*exp(-0.1894*t))
x2 = (1.00527*(exp(-9.925e-4*t)-exp(-0.1894*t)))
x3 = exp(-0.1894*t)

For the least squares fit, the objective is to minimize S = Σ(Ymeas - Ycalc)^2 summed over i = 1…n analyses

Taking the derivative of S with respect to each ai and setting this to zero leads to a series of equations that can be expressed in matrix form [C] = [X] [A] (subscripts i are omitted below)

$$[C] = \begin{matrix} \Sigma\ (x1*Ymeas) \\ \Sigma\ (x2*Ymeas) \\ \Sigma\ (x3*Ymeas) \end{matrix} \qquad [X] = \begin{matrix} \Sigma(x1\text{^}2) & \Sigma(x1*x2) & \Sigma(x1*x3) \\ \Sigma(x1*x2) & \Sigma(x2\text{^}2) & \Sigma(x2*x3) \\ \Sigma(x1*x3) & \Sigma(x2*x3) & \Sigma(x3\text{^}2) \end{matrix} \qquad [A] = \begin{matrix} a1 \\ a2 \\ a3 \end{matrix}$$

This is solved by finding the inverse [X]-1 so that [A] = [X]-1 [C]

The uncertainties in each term of [A] are found by first determining the standard error of measurement sy = sqrt(((1/(n-p))* Σ (ymeas - ycalc)^2) where n = number of data points, p = number of parameters = 3 in this case. This term sy is also the reduced Chi square for the equation. The uncertainties in each term are:
Sig(ai) = sy*sqrt(eii), where eii is a diagonal element of [X]-1

For the matrix inversion we need the determinant for matrix [X] and its adjoint. Each term in the adjoint is divided by the determinant to find the inverse.

The Excel routine creates a table of time, measured ^{220}Rn dpm and the elements for each xi. Subsequent columns are created for each of the products needed for summing to get terms in matrix [X]. The solutions for each activity term and its uncertainty are then displayed in a horizontal line. Each measurement has a weighting function that can be set to zero or 1. To assist in choosing weights, the ratio of computed activity to measured activity is displayed next to the measured value, with the ratio of counting uncertainty divided by measured value immediately next to this.

Estimating Uncertainty in Fitted Parameters from Counting Uncertainties

For the matrix calculation: $[A] = [X]^{-1}[C]$

Only the elements of [C] are influenced by the counting uncertainties.

For parameter $a1 = e_{11}*c_1 + e_{12}*c_2 + e_{13}*c_3$, where e_{ij} is an element of $[X]^{-1}$

The uncertainty in a1 should be $sig_{a1} = sqrt\ ((e_{11}*sigc_1)^2 + (e_{12}*sigc_2)^2 + (e_{13}*sigc_3)^2)$

Similar equations define a2 and a3

$c_j = \Sigma(x_{ji}*y_{imeas})$, where j = 1, 2, 3 and i is each data point.

Summing and error propagation leads to $sigc1 = sqrt\ (\Sigma(x_{1i}*sig_{yimeas})^2)$ with similar terms for sigc2 and sigc3

These are multiplied by the matrix elements above as shown, each term is squared, and the square root of the sum is taken to find the uncertainty in each parameter due to counting uncertainty (Crow et al., 1960).

3. **Methods used for reporting ^{228}Ra data**

As detailed in the main body of the manuscript, several methods were used to generate the ^{228}Ra dataset reported herein: gamma spectrometry and RaDeCC (A, A+B cartridges). The majority of the data were derived from the RaDeCC A cartridge method. Therefore, the table below summarizes the stations and depths where an alternative approach was used. Such alternatives were employed only where ^{228}Ra uncertainties were lower than the primary RaDeCC method.

Table SI-1. Methods used for deriving ^{228}Ra during the GEOTRACES GP15 cruise. Any station or depth not listed used the RaDeCC A cartridge ^{228}Th ingrowth method.

Station	**Depth(s)**	**Method**
3	45, 112, and 314 m	RaDeCC A+B
4	All depths	Gamma Spectrometry
5	All depths besides 3, 43, and 73 m	RaDeCC A+B
6	All depths besides 3, 348, 549, 747, and 999 m	RaDeCC A+B
8	1002, 1301, 1891, 1903, 2292, 3996, 4497, 4996, and 5047 m	RaDeCC A+B
10	1221, 2734, 3485, 4885, and 5044 m	RaDeCC A+B
12	1100, 1900, and 2750 m	RaDeCC A+B
12	4500, 5425, 5505, and 5545 m	Gamma Spectrometry
14	2300, 4500, and 5165 m	RaDeCC A+B
16	1250, 3000, 4000, 5205, 5285, 5325 m	RaDeCC A+B
18	4250 and 4750 m	RaDeCC A+B
18.3	All depths besides 3 and 500 m	RaDeCC A+B
19	3500, 4970, 5050, and 5090 m	RaDeCC A+B
21	3250, 4250, 5218, 5298, and 5338 m	RaDeCC A+B
23	2450, 2600, 2900, and 3500 m	RaDeCC A+B
25	1569, 1961, and 3499 m	RaDeCC A+B
37	All depths	Gamma Spectrometry
39	All depths	Gamma Spectrometry

4. MATLAB code for processing RaDeCC data

Co-author Doug Hammond developed a Matlab routine to open RadeCC files, read the data out, analyze it, and summarize results. In this study, samples were counted between 180 minutes and sometimes up to a full day. The Matlab program allows the user to select the length of time to include in the calculation. It is more comprehensive than the excel file approach that most RaDeCC users have used in the past, which relies upon a constant counting length for all samples and entered the data as a single line.

However, the Matlab program has an additional important feature. It takes each line of data from the file, does chance counts corrections for the line to find corrected activity in each window, and then plots the data. This allows visualization of whether there are time trends of significance, particularly if count rates decline due to leakage of air into the sample or perhaps build-up of water during the count. After chance coincidence corrections are done, an average of individual line results can be done, with the uncertainty calculated from the variance of each line from the mean. We argue that this is a better way to assess uncertainty than propagating errors from counting statistics and solves a non-linearity problem discussed below.

For the 220 window we have observed increases in data noise with time. The program allows the user to review the trend for each file and decide on the counting duration to use. Alternatively, the program calculates the slope and slope uncertainty for 219, 220 and total cpm channels. These parameters can be used to screen out problematic samples when leakage or water might have been a problem. This tends to be a larger problem for the 220 channel due to its much higher sensitivity to chance counts. Lastly, the program corrects for channel cross-talk using the average count rates for 219 and 220 to give a final corrected cpm for each window.

The program has been verified based on checks vs the Excel approach. The results for the 219 channel are nearly identical. However, the corrected 220 cpm results differ because the effect of increasing count rates on chance coincidence is non-linear. When an interval of 180 or 300 minutes is used, the non-linearity introduces an error of several percent or more, depending on activity, because the Excel approach assumes the total cpm is constant for the time block used. When multiple short intervals are used in the program, the change in total cpm during an interval is small and the non-linearity effect does not show up.

This last file also rejected two of the intervals used by the excel file, due to noise flagged by the Matlab routine. The criteria used for noise rejection is a count rate more than 3.5 sample standard deviations from the mean and sample standard deviation for the intervals chosen (the noisy intervals were about 5 ssds from the mean for 219; the 220 calculation did not include the rejected intervals).

The Matlab code can be downloaded here https://github.com/dhammond90290/RadeccMatlab/blob/main/. This program was written for a Mac. If a PC is used, there is a backslash that must be changed (see comments in RadeccFolder).

Raw RaDeCC files for processing need to be added into a folder that contains the Matlab application. There will be 3 Matlab routines in the Matlab folder, as well as the data folder:

(1) LLSQ (a function that does a linear fit to y=mx+b and computes uncertainties in m and b)
(2) RadeccWorkupX (this reads each file and does the calculation for the file, putting results in a variable 'Output', where X=the latest version of the code)
(3) RadeccFolder (this runs the data reduction for a batch of files in the folder, using the two functions above)

Instructions are provided as the program runs and there are numerous comments embedded within the code that allow the user to understand how it works and make their own modifications if desired. In brief, it shows results for each window and asks what intervals to use for data reduction. This could be changed to do a large batch with pre-specified criteria. The results are diverted into a variable called Output. The user needs to open this variable when the calculations are done, copy the elements and paste them into an excel spreadsheet.

5. Measurement of ^{228}Ra on B cartridges.

The B cartridges were not measured at sea. The initial measurement was used to set the initial ^{228}Th derived from seawater. A later measurement was used to evaluate the amount of ^{228}Th that had been produced from ^{228}Ra decay. Here are the details of this procedure.

The measurement of ^{228}Ra adsorbed to Mn-cartridges is based on the decay over time of ^{228}Ra to ^{228}Th. When the sample is collected it contains both ^{228}Ra and ^{228}Th that were dissolved in seawater. Over time ^{228}Ra decay produces new ^{228}Th while ^{228}Th adsorbed from seawater decreases. By measuring ^{228}Th two times we can calculate $^{228}_{i}$Ra according to the equation

$$^{228}_{i}Ra \pm stdev = \frac{(^{228}_{m}Th \pm stdev) - \left((^{228}_{i}Th \pm stdev) * e^{[-\lambda_{Th} t_1]}\right)}{1.499 * \left(e^{[-\lambda_{Ra} t_1]} - e^{[-\lambda_{Th} t_1]}\right)} \quad (1)$$

Here $^{228}_{i}$Ra is initial ^{228}Ra at the time of the first ^{228}Th measurement ($^{228}_{i}$Th), $^{228}_{m}$Th is the measured ^{228}Th during the second measurement, t_1 is the elapsed time between measurements, and stdev is the standard deviation of the measurement.

We can then calculate ^{228}Ra at the time of sample collection ($^{228}_{col}$Ra)

$$^{228}_{col}Ra \pm stdev = \frac{^{228}_{i}Ra \pm stdev}{\left(e^{[-\lambda_{Ra} t_2]}\right)} \quad (2)$$

Here t_2 is the elapsed time between sample collection and the time of the first ^{228}Th measurement.

6. Combining GP15 data with published data in the region of the North Pacific Current (NPC).

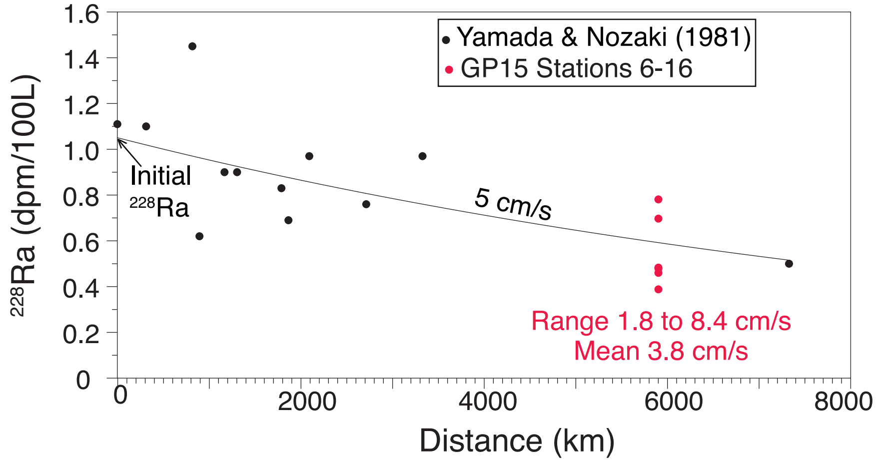

Figure SI-1. Black dots are surface data reported by Yamada and Nozaki (1986) and Nozaki et al. (1998) between 143°E (500 km off the Japan coast) to 136.3°W. This curve indicates an initial ^{228}Ra activity of 1.05 dpm/100L 500 km off the Japan coast. If we assume this is a steady state line source and only advection and decay control the decrease of ^{228}Ra, the average current speed is 3.8 cm/s, very similar to the offshore velocity reported by Aoyama et al. (2016). The red dots indicate the average ^{228}Ra activities in the upper 100 m of the water column at GP15 stations 6-16 (27-52°N, 152°W).

7. Puna Ridge

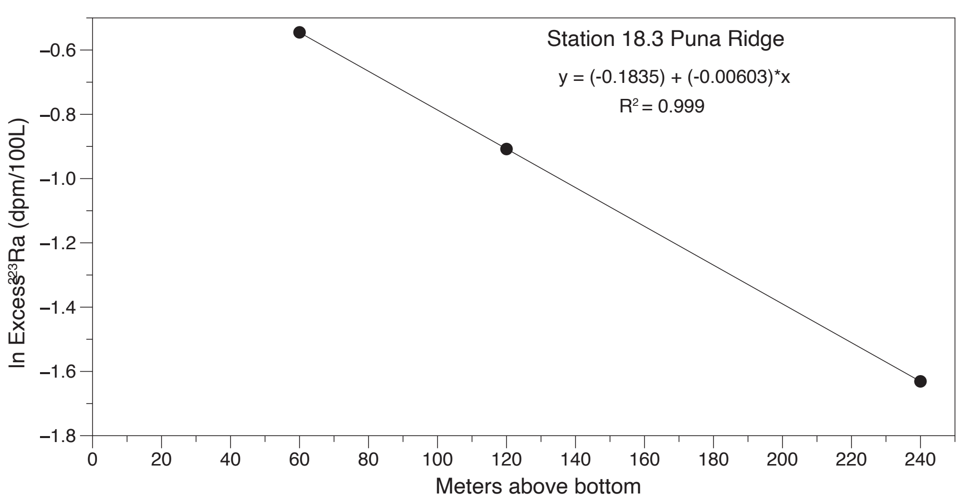

Figure SI-2. Activities of ^{223}Ra in the three deepest samples at Station 18.3 (Puna Ridge) follow a strong exponential decrease when plotted against distance above bottom.

The term (λ/K_z) in equation 3 is obtained by plotting measured ln ^{223}Ra as a function of distance above bottom (Figure SI-2). Because ^{223}Ra in samples collected more than a few hundred meters above bottom may be diluted by horizontal advection, we restrict our data set to 3 samples collected within 120 m of the bottom. Here the slope of the line (-0.00603) is the square root of (λ/K_z). Solving for K_z yields a vertical mixing rate of 0.019 m^2/s.

8. Depth profiles for each station

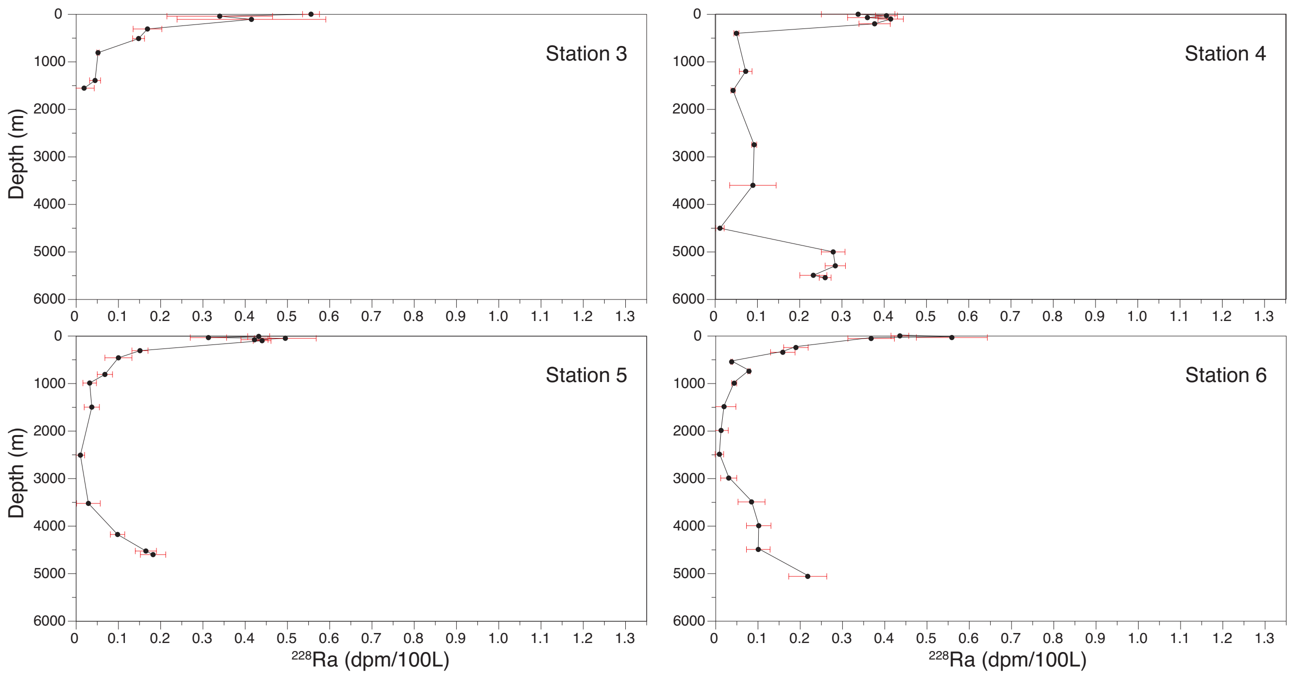

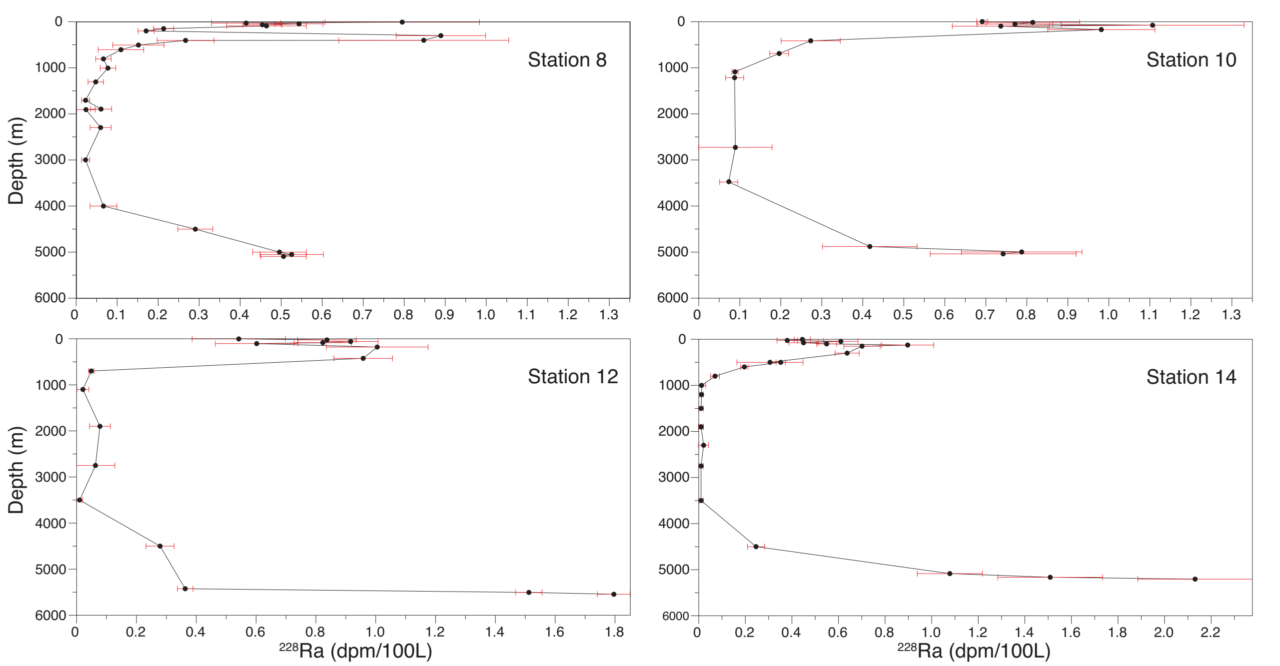

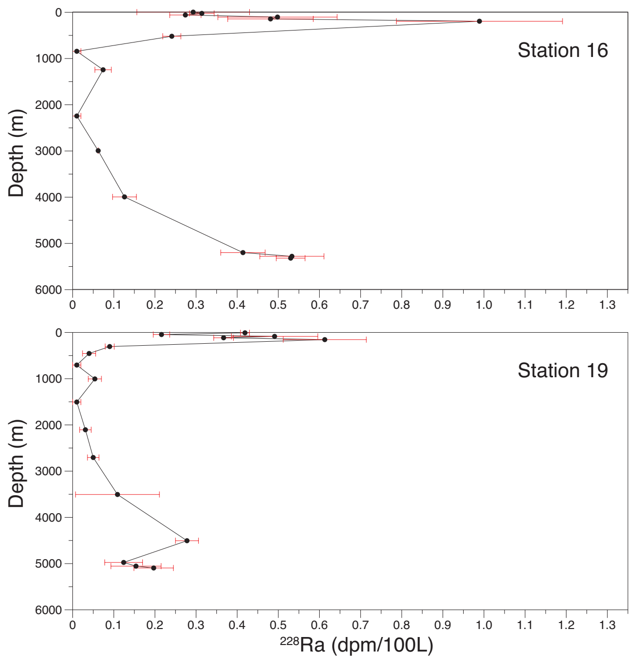
Station 16
Station 18
Station 19
Station 21
Depth (m)
0
1000
2000
3000
4000
5000
6000
0 0.1 0.2 0.3 0.4 0.5 0.6 0.7 0.8 0.9 1.0 1.1 1.2 1.3
^{228}Ra (dpm/100L)

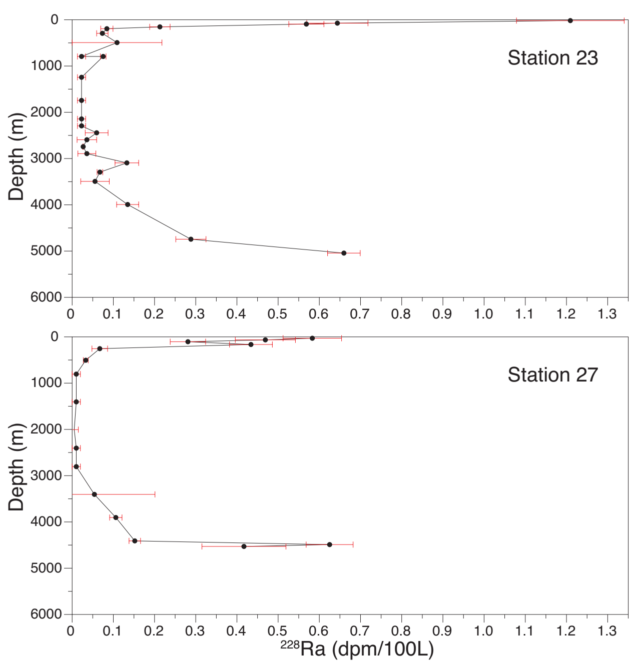
Station 23
Station 25
Station 27
Station 29
Depth (m)
0
1000
2000
3000
4000
5000
6000
0 0.1 0.2 0.3 0.4 0.5 0.6 0.7 0.8 0.9 1.0 1.1 1.2 1.3
^{228}Ra (dpm/100L)

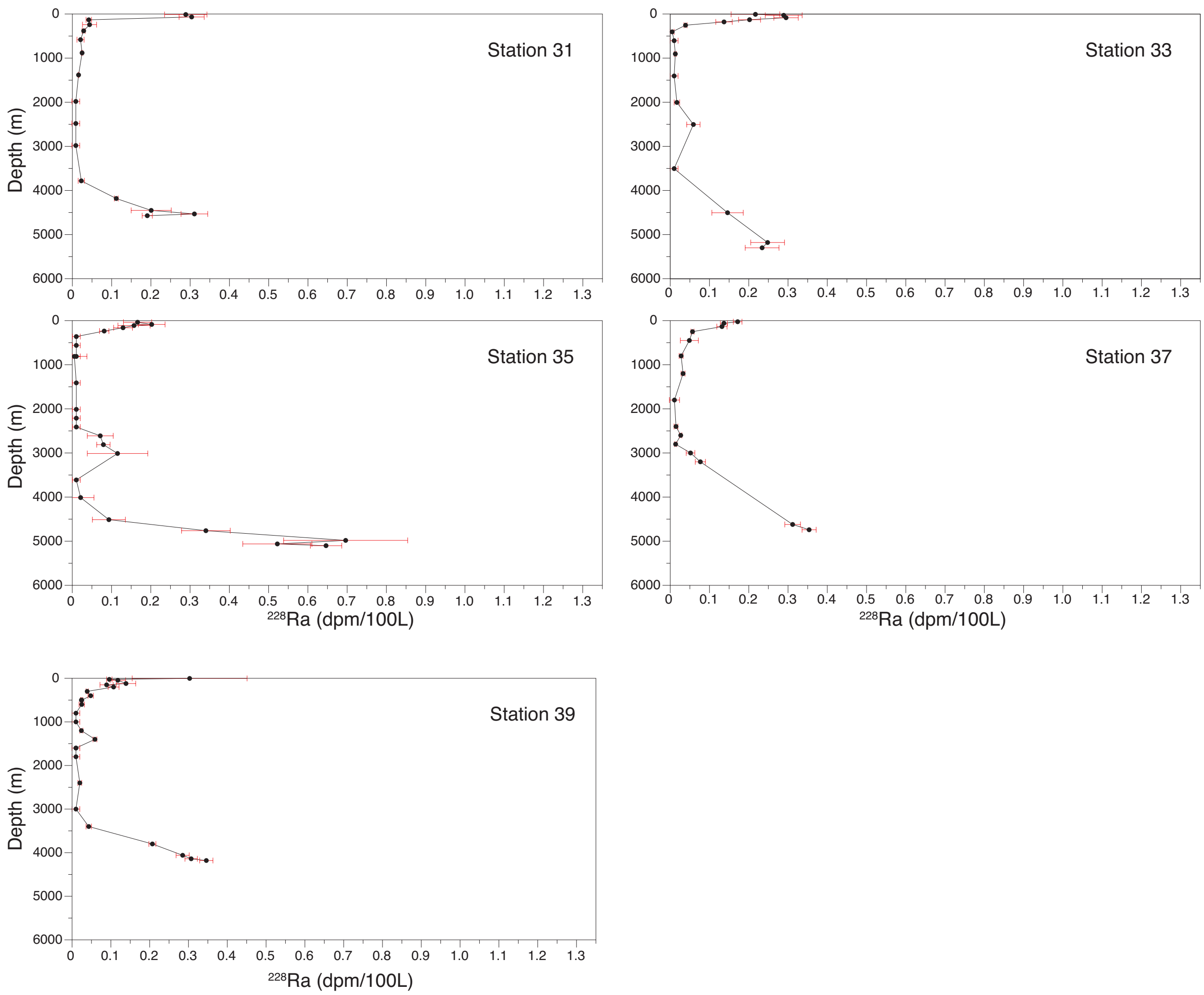

Figure SI-3. Depth profiles of ^{228}Ra (dpm/100L) stations 3-39. Error bars are 1 sigma.

10. SI References

Aoyama, M., Hamajima, Y., Inomata, Y., Kumamoto, Y., Oka, E., Tsubono, T., Tsumune, D., 2018. Radiocaesium derived from the TEPCO Fukushima accident in the North Pacific Ocean: surface transport processes until 2017. J. Environ. Radioact. 189, 93–102.

Charette, M.A., Morris, P.J., Henderson, P.B., Moore, W.S., 2015. Radium isotope distributions during the US GEOTRACES North Atlantic cruises. Mar. Chem. 177, 184–195. doi:10.1016/j.marchem.2015.01.001

Crow, E.L., F. A. Davis, M.W. Maxfield (1960), Statistics Manual, Dover Publ. 288pp.

Key, R.M., Brewer, R.L., Stockwell, J.H., Guinasso, N.L., Schink, D.R., 1979. Some improved techniques for measuring radon and radium in marine sediments and in seawater. Mar. Chem. 7, 251–264. doi:10.1016/0304-4203(79)90042-2

Nozaki, Y., Dobashi, F., Kato, Y., Yamamoto, Y., 1998. Distribution of Ra isotopes and the 210Pb and 210Po balance in surface seawaters of the mid Northern Hemisphere. Deep Sea Res. Part I Oceanogr. Res. Pap. 45, 1263–1284.

Yamada, M., Nozaki, Y., 1986. Radium isotopes in coastal and open ocean surface waters of the Western North Pacific. Mar. Chem. doi:10.1016/0304-4203(86)90057-5